

Analytical Modelling of Surface Roughness during Compacted Graphite Iron Milling Using Ceramic Inserts

Ş. Karabulut, A. Güllü, A. Gültaş, R. Gürbüz

Abstract—This study investigates the effects of the lead angle and chip thickness variation on surface roughness during the machining of compacted graphite iron using ceramic cutting tools under dry cutting conditions. Analytical models were developed for predicting the surface roughness values of the specimens after the face milling process. Experimental data was collected and imported to the artificial neural network model. A multilayer perceptron model was used with the back propagation algorithm employing the input parameters of lead angle, cutting speed and feed rate in connection with chip thickness. Furthermore, analysis of variance was employed to determine the effects of the cutting parameters on surface roughness. Artificial neural network and regression analysis were used to predict surface roughness. The values thus predicted were compared with the collected experimental data, and the corresponding percentage error was computed. Analysis results revealed that the lead angle is the dominant factor affecting surface roughness. Experimental results indicated an improvement in the surface roughness value with decreasing lead angle value from 88° to 45°.

Keywords—CGI, milling, surface roughness, ANN, regression, modeling, analysis.

I. INTRODUCTION

COMPACTED Graphite Iron (CGI) is considered to be a potential alternative for flake graphite iron for manufacturing new generation high-power diesel engines. Use of CGI, which is characterized by higher strength and stiffness, allows an engine to perform at higher peak pressure with higher fuel efficiency and lower emission rate. Given these advantages, CGI is considered to be an important manufacturing material and is being widely used as an alternative for Grey Cast Iron (GCI) in the automotive industry for the production of several parts, including engine heads, diesel engine blocks, exhaust manifolds and brake discs. Additionally, this material facilitates higher pressure in the chamber, thereby leading to more efficient fuel combustion. However, CGI has poor machinability when compared with GCI, resulting in higher cutting tool wear and loss in productivity [1]-[5]. Recently, several studies have used neural networks for predicting and optimizing the cutting parameters during milling operations to obtain desired responses such as cutting force, surface roughness and tool

wear. For instance, Tsai et al. developed an artificial neural network (ANN)-based surface recognition system to predict the surface roughness of machined parts during the end milling process. Such an approach is expected to assure product quality and increase the production rate by predicting the surface finish parameters in real time. Experimental results show that the proposed ANN-based surface recognition model exhibits a high accuracy rate (96%–99%) for predicting surface roughness under a variety of combinations of cutting conditions [6]. Furthermore, Zain et al. presented an ANN-based model for predicting surface roughness during the machining process. On the basis of the predictions, the recommended combination of cutting conditions to obtain the best surface roughness value is high speed with low feed rate and radial rake angle [7]. Alauddin et al. developed mathematical models for predicting the surface roughness using speed and feed. The surface roughness contours thus obtained could select a combination of parameters for realizing machining time reduction without increasing the surface roughness [8]. Benardos et al. presented a neural network model for predicting the surface roughness during CNC face milling. The proposed ANN-based method predicted the surface roughness with a mean squared error of 1.86%. According to that study, for the given surface roughness, tool and work piece, it is necessary to determine the optimum cutting condition [9]. Bajic, Lela and Zivkovic examined the influences of various cutting parameters, including cutting speed, feed rate and depth of cut, on the surface roughness during face milling using ANNs. According to their study, the neural network model provides a better explanation of the observed physical system. Accordingly, the optimal cutting parameters were determined using the simplex optimization algorithm [10]. Munoz et al. [11] experimentally investigated the surface milling of A1 7075-T7351 and modelled the experimental results using ANNs. Their experiments have shown that there is a strong correlation between chip thickness and surface roughness. Chien and Chou developed a mathematical model for determining the machinability of type 304 stainless steel during an experiment. The surface roughness, cutting power and tool life was predicted to be 4.4%, 5.3% and 4.2%, respectively [12]. Sağlam applied and evaluated ANNs in his experiment to establish an observation system for a smart tool status on the basis of the results of cutting powers during face milling operations. The tool wear and surface roughness were predicted with a success rate of 77% and 79%, respectively [13]. Lo indicated that ANN-based models are highly effective in metal cutting applications. According to that study, factors

Ş. Karabulut is with Department of Mechanical Program, Hacettepe University, 06935 Turkey (corresponding author to provide phone: 505-562-0991; fax: 312-267-3338; e-mail: senerkarabulut@hacettepe.edu.tr).

A. Güllü and A. Gültaş are with the Manufacturing Engineering Department, Gazi University, Faculty of Technology, Turkey (e-mail: agullu@gazi.edu.tr, aguldas@gazi.edu.tr).

R. Gürbüz is with the Department of Mechanical Program, Karatekin University, 18200 Cankiri, Turkey (e-mail: rizagurbuz@karatekin.edu.tr).

such as radius of the cutting tool edge, feed rate, cutting speed, heat and vibrations are the main parameters influencing surface roughness [14]. Öktem et al. established a mathematical model with ANNs to investigate the surface roughness values during the milling of type AISI 1040 steel in wet cutting with carbide tools [15]. Asiltürk et al. studied the effect of cutting parameters on surface roughness (R_a) during the machining of AISI 1040 hardened steel. Experimental results indicated that the feed rate is the most important parameter among the different parameters influencing surface roughness [16]. Kivak determined the effects of the machining parameters on the surface roughness and flank wear by the analysis of variance (ANOVA). The analysis results showed that feed rate is the dominant factor affecting surface roughness, whereas flank wear is significantly influenced by cutting speed [17].

Surface roughness essentially describes the surface geometry of the machined part. Controlling the surface roughness of any manufacturing process has become a critical factor because of the increased demands on the quality of the final product. Surface roughness is not only an important measure of the quality of a product but also influences the production cost significantly. The main objective of this study is to investigate the influence of lead angle variation and cutting conditions on surface roughness. To this end, experiments were performed under dry machining conditions and an ANN-based prediction model was developed to predict the effect of lead angle and maximum chip thickness on the surface roughness while machining CGI under various cutting parameters, such as cutting speed, feed rates and constant depth of cut.

II. EXPERIMENTAL PROCEDURES

A. Characteristics of the Work Pieces

In this study, we used rectangular CGI blocks of dimension $100 \times 100 \times 100$ mm. This material was selected for the experimental research, considering the fact that it is being widely employed in the automotive industry for the production of engine heads, diesel engine blocks, exhaust manifolds and brake discs. Given its increased strength when compared with the traditional GCI, it allows an increase in the cylinder pressure, a better fuel economy and a higher power output. In the typical process, CGI blocks were mounted with M10 screws on the dynamometer and were face milled by the down milling method (Fig. 1). Fig. 2 shows the microstructure of CGI used in the experiment. As is observed, the surface of the CGI has several individual worm-shaped particles, which are shorter and have a rounded edge. Additionally, the CGI has some spheroidal graphite particles. These particles provide superior mechanical properties to the CGI, and are responsible for increasing the strength and stiffness [4]. Table I. summarizes the chemical composition of the CGI specimen as obtained during the casting process in the factory. The mechanical properties of the CGI are listed in Table II.

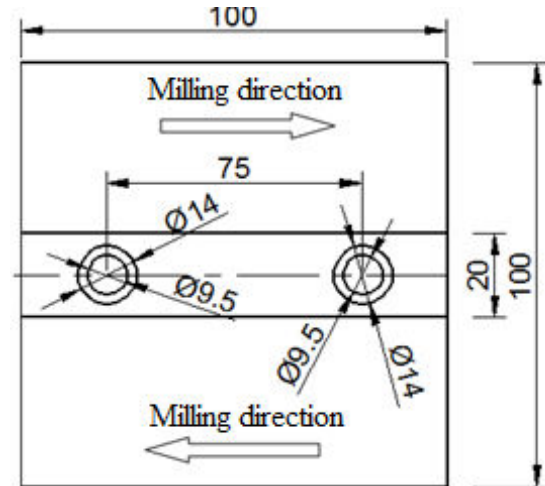


Fig. 1 Specimen for measuring cutting force [18]

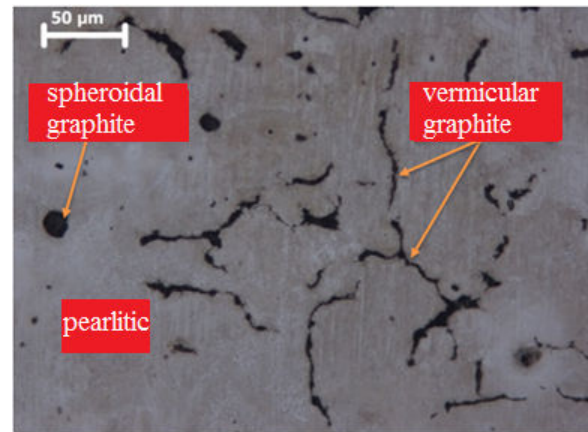


Fig. 2 Microstructure of CGI

TABLE I
 CHEMICAL COMPOSITION OF CGI

C	Si	Mn	P	S	Cr	Ni	Mo
3,82	1,804	0,337	0,031	0,015	0,074	0,013	0,002
Cu	Mg	Sn	Ti	Al	Zn	Bi	Fe
0,879	0,014	0,092	0,0203	0,008	0,082	0,007	Bal.

TABLE II
 MECHANICAL PROPERTIES OF CGI

Ultimate Tensile Strength (MPa)	%0.2 Yield Strength (MPa)	Elongation (%)	Typical Hardness, HV	Impact test (Joule)
502,7	284,3	1,8	280,0	8,6

B. Machining Tool, Cutting Insert and Roughness Measurements

The face milling operation was performed using a Johnford VMC550 model three-axis CNC milling machine tool under dry cutting conditions. A standard 63 mm tool holder with two cutting edges (insert) was used in the experiments. Sandvik coromant CC6090 quality Si₃N₄-based (Sialon) ceramic inserts with ISO code R245-12 T3 E 6090 were mounted on the tool holder. The average surface roughness (R_a) of the workpiece was measured on a MAHR-Perthometer M1 portable surface roughness device. Every surface was

machined with a separate set of tools. The surface roughness was measured by machining the samples along 100 mm, and the average values were calculated by measuring the rate of surface roughness at 4 different points.

C. Cutting Parameters

For the experimental study, the lead angle, cutting speed and maximum chip thickness were selected as variables. The three variables for maximum chip thickness, namely, 0.07, 0.084 and 0.1008 were determined from the tool supplier catalogue. The feed rate f_z was continuously changed in connection with the equation $h_{ex} = f_z \times \sin \kappa_r$. Accordingly, 48 different feed rates were used in the experiments. The feed rates were increased while reducing the lead angle. The cutting parameters used in the experiments are shown in Table III.

TABLE III
 CUTTING PARAMETERS USED IN THE EXPERIMENTS

Parameters	Values
Lead angles (Degree), κ_r	45°, 60°, 75°, 88°
Cutting speed (m/min), V_c	334, 400, 460, 530
Maximum chip thickness (mm), hex	0.07, 0.084, 0.1008
Depth of cut (mm), ap	2.5
Cutting width (mm), ae	40
Tool holder diameter (mm), D_c	63
Number of cutting edge, Z_n	2

III. MODELING OF SURFACE ROUGHNESS VALUE

A. Estimation of Surface Roughness Value Using ANN

The surface roughness was estimated using a feed-forward four-layered back propagation neural network, as shown in Fig. 3. A multilayer ANN model with back propagation was specifically chosen in this experiment because of its wide application and the use of the Levenberg–Marquardt algorithm. The network was constructed with four layers, including the input, output and hidden layers. The ANN with one hidden layer gave significantly high errors; hence, a two-layer network was considered. The input neurons are cutting speed, various lead angles and chip thickness, whereas the output neuron is surface roughness (Ra). Pythia software was used for training this network, and the ANN was trained with the back propagation algorithm. The software randomly selected the weights of the network connections. The neural network was trained with 32 experimental data and was subsequently validated and tested with 16 experimental data. The prediction performance of the ANN model developed in the experimental study was specified in terms of the coefficient of determination (R^2), root mean square error (RMSE) and mean absolute percentage error (MAPE).

$$R^2 = 1 - \frac{\sum (Ra_i - Ra_{ANN,i})^2}{\sum (Ra_{ANN,i})^2} \quad (1)$$

$$RMSE = \sqrt{\left(\frac{1}{n} \sum_{i=1}^n |Ra_{ANN,i} - Ra_i|^2 \right)} \quad (2)$$

$$MAPE = \sqrt{\left(\frac{1}{n} \sum_{i=1}^n \left| \frac{Ra_{ANN} - Ra_i}{Ra_{ANN}} \right| \times 100 \right)} \quad (3)$$

The Pythia software uses Fermi function as the transfer function. The input and output values are normalized in (-1,1). Table IV summarizes the maximum and minimum values of the cutting parameters used in the experiment for normalization. The Fermi transfer function can be measured using (4):

$$N(z) = \frac{1}{1 + e^{-4(z-0.5)}} \quad (4)$$

The experimental results were trained with ANN and were investigated with the most appropriate network structures, different cycle and neuron counts. First, a network structure with the lowest deviation value was selected by automatically optimizing the software. After specifying the network structure, it was trained up to the smallest deviation value by changing the deviation count and training values of the software. Following these operations, a network structure comprising four layers and nine neurons was selected for the experiments.

TABLE IV
 THE LIMIT VALUES FOR ANN SOFTWARE

	Inputs		
	Lead angle (κ_r)	Cutting speed (Vc)	Table feed speed (Vf)
Maximum	88	530	764
Minimum	45	334	237

To test the reliability of the network structure, the real values were compared with the results of the network structure. The results indicate no explicit error in the deviation rate. After this phase, the weight values in the neurons were imported into the Excel software. Following that, an analytical model was developed with these weight values so as to predict the average surface roughness value (Ra).

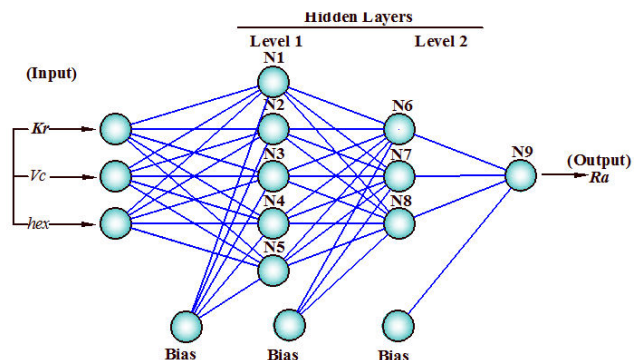


Fig. 3 ANN structure in the LM algorithm with nine neurons

ANNs consist of a number of elementary units called neurons. A neuron is a simple processor, which takes one or more input values and produces an output. Each input value is multiplied with the weight values connected with it. The weighted input values are added linearly to obtain the output

values. As shown in Fig. 3, the output values thus obtained are used as input values for other neurons. Equation (5) was acquired using the weight values of the neurons in the ANN network structure during the milling conditions. This equation can be used for predicting the surface roughness value (Ra) while milling the compacted graphite iron using the ceramic inserts.

$$N_{9(Ra)} = \frac{1}{1 + e^{-4(-2.986773 \cdot N_6 + 1.403399 \cdot N_7 + 1.625655 \cdot N_8 - 0.5)}} \quad (5)$$

The Fermi transfer function is expressed as

$$N_{(i)} = \frac{1}{1 + e^{-4 \cdot (E_i - 0.5)}} \quad (6)$$

TABLE V
 CONSTANTS USED IN (7) FROM NEURONS 1-5

i	Constants		
	w1i	w2i	w3i
1	-0.200544	-0.785645	-0.825014
2	0.685859	-0.871897	1.432073
3	-0.650129	-2.109688	0.680974
4	0.695588	-0.437300	-1.744061
5	0.634416	0.409598	-0.539687

The E_i value was calculated using (7) for the neurons from N1 to N5. Here i represent the neuron numbers in the equation. The obtained weights are shown in Table V.

$$E_i = w_{1i} \cdot V_c + w_{2i} \cdot K_r + w_{3i} \cdot V_f \quad (7)$$

Similarly, the E_i value for the neurons from N6 to N8 was calculated using (8). The obtained weights are shown in Table VI.

$$E_i = w_{1i} \cdot N_1 + w_{2i} \cdot N_2 + w_{3i} \cdot N_3 + w_{4i} \cdot N_4 + w_{5i} \cdot N_5 \quad (8)$$

TABLE VI
 6-8 CONSTANTS USED IN (8) FROM NEURONS 6-8

i	Constants				
	w1i	w2i	w3i	w4i	w5i
6	1.63678	-1.68025	3.46102	1.20995	0.37378
7	-0.93867	0.12453	0.11363	1.14585	0.41122
8	0.32120	0.00415	0.93702	-2.15098	0.69684

B. Estimation of Surface Roughness by Regression Analysis

In this study, regression analysis was also used for modelling and analysing the several cutting variables, where there is relationship between the dependent and independent variables. The dependent variable is surface roughness (Ra), whereas lead angle (K_r), cutting speed (V_c) and maximum chip thickness (hex) are the independent variables. The linear regression model was generated under the main effects of control factors, and the coefficient of determination for this equation was calculated as $R^2 = 0.924$. This result was realized under the confidence level of 95%. Hence, the predictive equations for the quadratic regression of surface roughness were calculated with factor interactions.

$$Ra = 0,0866371 + 0,00344224 \times K_r - 0,0000879685 \times V_c + 0,00023951 \times V_f \quad (9)$$

The coefficient of determination for the quadratic equation was calculated as $R^2 = 0.95$ and is given as follows:

$$Ra = -0,244888 + 0,00604697 \times K_r + 0,000326014 \times V_c + 0,000990923 \times V_f + 0,0000101646 \times K_r \times K_r - 0,000000800118 \times V_c \times V_c - 0,00000054651 \times V_f \times V_f \quad (10)$$

The equations show that the surface roughness value increases with increasing lead angle, cutting speed and maximum chip thickness. Among these cutting parameters, the lead angle (K_r) has the most dominant effect on the surface roughness. As the lead angle increases from 45° to 88° , there is an increase in the cutting tool vibration. This often leads to the formation of micro-cracks on the cutting insert, thereby contributing to an increase in the surface roughness value.

IV. RESULTS AND DISCUSSIONS

In the experiments, the surface roughness was affected by the cutter lead angle and maximum chip thickness. Experimental results indicate that the surface roughness value improves with decreasing lead angle from 88° to 45° . The highest surface roughness value of $Ra = 0.47 \mu\text{m}$ was obtained for the cutting parameters of $K_r = 88^\circ$, $V_c = 530 \text{ m/min}$ and $V_f = 540 \text{ mm/min}$. The best surface roughness value of $Ra = 0.26 \mu\text{m}$ was obtained for $K_r = 45^\circ$, $V_c = 334 \text{ m/min}$ and $V_f = 334 \text{ mm/min}$. The main effects of the control factors were evaluated using the variance analysis. Accordingly, the effects of the control factors on the surface roughness during the experiments are as follows: lead angle (K_r) 73.79%, feed rates (hex) 14.25%, cutting speed (V_c) 4.42% and product of cutting speed and feed rate ($V_c \times V_f$) 2.19%. The results of the variance analysis, as shown in Table VII, indicate that the lead angle has the greatest effect on the surface roughness when machined under different lead angles, while the cutting speed has the least effect. The surface roughness value increased, in addition to the increase in feed rate value as a function of the maximum chip thickness (hex). The experimental results obtained in this study were realized in parallel to the related literature. With increase in the lead angle from 45° to 88° for a given chip thickness, the cutting tool vibration and micro-cracks increased on the cutting edge during the cutting process. Consequently, there was an associated increase in the surface roughness value. After completing the ANN training and regression analysis, the ANN and regression analysis equations were tested using the experimental results. For this, the experimental results were graphically compared with the results obtained from the training network and regression analysis equation. The scatter diagrams of the predicted and measured values of the surface roughness values are shown in Fig. 5. The coefficients of determination R^2 for ANN and regression analysis were found to be 0.9784 and 0.95, respectively. Fig. 6 shows the comparison of the predicted and measured values of the surface roughness values for a set of 16 testing data after obtaining the mathematical equations

using ANN and regression analysis. As is observed, the predicted surface roughness values are very close to the measured values for all the cutting parameters. The prediction

rate using ANN and regression analysis was found to be 94.27% and 97.74%, respectively.

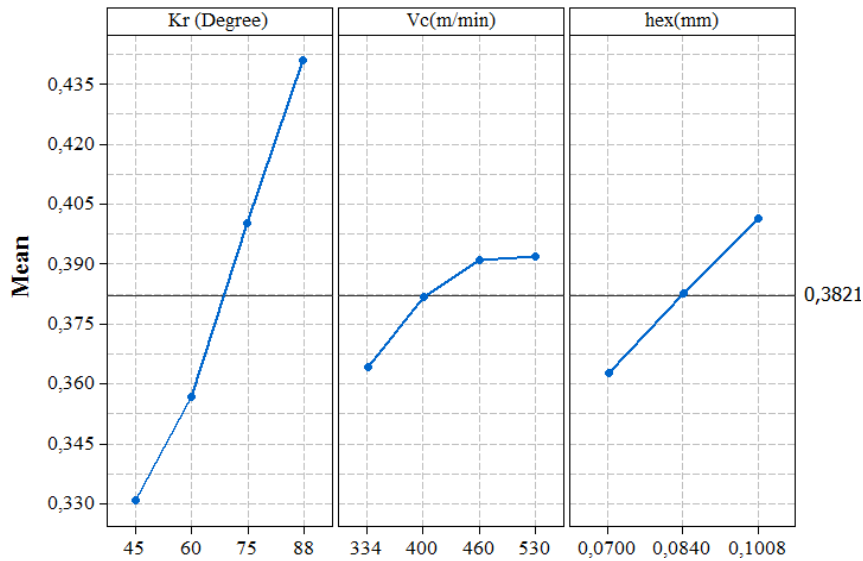


Fig. 4 Effects of the cutting parameters on the surface roughness

TABLE VII
 ANALYSIS OF VARIANCE (ANOVA)

Source	DF	SS	MS	F	P	Effect rate (%)
Kr	1	0.0568110	0.0010466	5.9774	0.022961	73.79%
Vc	1	0.0034038	0.0000459	0.2623	0.613635	4.42%
Vf	1	0.0109723	0.0012201	6.9684	0.014963	14.25%
Kr*Vc	1	0.0000049	0.0000379	0.2162	0.646493	0.01%
Kr*Vf	1	0.0000583	0.0001964	1.1218	0.301029	0.08%
Vc*Vf	1	0.0016925	0.0000057	0.0328	0.858015	2.20%
Kr*Kr	1	0.0000035	0.0000685	0.3911	0.538152	0
Vc*Vc	1	0.0000445	0.0001571	0.8971	0.353845	0.06%
Vf*Vf	1	0.0001448	0.0001448	0.8271	0.372978	0.19%
Error	22	0.0038519	0.0001751			5.00%
Total	31	0.0769875				

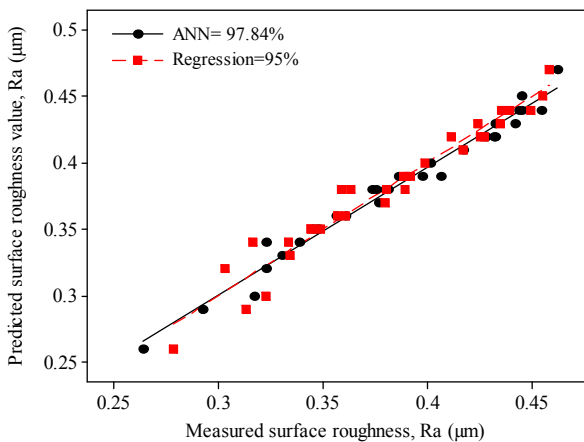


Fig. 5 Comparison of training data result with the ANN model and regression model

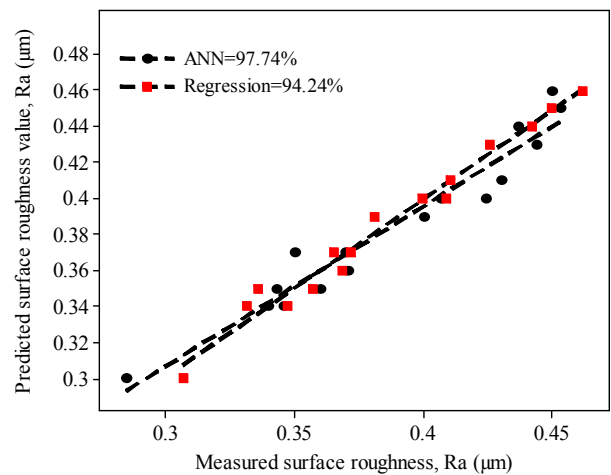


Fig. 6 Comparison of test data with the prediction model

V. CONCLUSIONS

In this study, CGI was milled under various lead angles and cutting parameters using ceramic cutting inserts. The ANN was initially trained with 32 experimental data. Following that, the reliability of the ANN model was tested with 16 experimental data under dry cutting conditions. Furthermore, the experimental results were evaluated using ANOVA. The following conclusions could be inferred from the results:

There existed a strong correlation between the surface roughness value and lead angle in each trial of the experiment. Experimental results during the milling of CGI using ceramic inserts showed that the surface roughness values improve with decreasing lead angle. More specifically, on decreasing the lead angle from 88° to 45°, there is an increase in the feed rate and the volume of the removed chip. This situation, in general, has a negative impact on the surface roughness. Intriguingly, however, the surface roughness value improved at a smaller lead angle. With increasing lead angle from 45° to 88° for a given chip thickness, there is an increase in the cutting tool vibration. This often leads to the formation of micro-cracks on the cutting edge. As a result, the value of surface roughness increases correspondingly. For optimum surface roughness during the machining of CGI using ceramic inserts, it is recommended to perform the face milling operation at cutting speed within the range 334 to 400 m/min, lead angle within the range 45° to 60° and maximum chip thickness of 0.07 mm.

The mathematical model indicated a good agreement between the experimental data and predicted values for surface roughness. According to the ANOVA results, the lead angle is the most significant parameter influencing the surface roughness, with a percentage contribution of 73.79%. According to the confirmation test results, the measured values are within the 95% confidence interval. The R2 values of the ANN and regression analysis for the confirmation data were calculated as 94.27% and 97.74%, respectively. These results indicate beyond ambiguity that the ANN-based model is reliable and accurate in successfully modelling the surface roughness during the face milling of CGI.

ACKNOWLEDGMENTS

The authors would like to thank TUBİTAK and Compenanta DÖKTAŞ for their support in this work.

REFERENCES

- [1] Nayyar, V.; Zubayer, A.; Jacek, K.; Anders, K.; Lars, N. An Experimental Investigation of the influence of cutting-edge geometry on the machinability of compacted graphite iron. *IJMMME* 2013, 3.1, 1–25.
- [2] Hick, H.; Langmayr, F. All-star cast. *Engine Technology International Conference (January)* 2000, 40–42.
- [3] Marquard, R.; Helfried, S.; McDonald, M.C. New materials create new possibilities. *Engine Technology International* 1998, 2, 58–60.
- [4] Guesser, W.; Schroeder, T.; Dawson, S. Production experience with compacted graphite iron automotive components. *AFS Transactions, DesPlaines* 2001.
- [5] Abele, E.; Schramm, B. Wear behaviour of PCD in machining. *Proceedings of the 2nd Industrial Diamond Conference, Rome* 2007.
- [6] Tsai, Y.H.; Chen, J.C.; Luu, S.J. An in-process surface recognition system based on neural networks in end milling cutting operations.

- [7] Zain, A.M.; Haron, H.; Sharif, S. Application of GA to optimize cutting conditions for minimizing surface roughness in end milling machining process. *Expert Systems with Applications* 2010, 37, 4650–4659.
- [8] Alauddin, M.; El Baradie, M.A.; Hashmi, M.S.J. Optimization of surface finish in end milling inconel 718. *Journal of Materials Processing Technology* 1996, 56, 54–65.
- [9] Benardos, P.G.; Vosniakos, G.C. Prediction of surface roughness in CNC face milling using neural networks and Taguchi's design of experiments. *Robotics and Computer-Integrated Manufacturing* 2002, 18, 343–354.
- [10] Bajic, D.; Lela, B.; Zivkovic, D. Modeling of machined surface roughness and optimization of cutting parameters in face milling. *Metalurgija* 2008, 47, 331–334.
- [11] Munoz-Escalona, P.; Maropoulos, P.G. Artificial neural networks for surface roughness prediction when face milling Al 7075–T7351. *Journal of Materials Engineering and Performance* 2010, 19, 185–193.
- [12] Chien, W.T.; Chou, C.Y. The predictive model for machinability of 304 stainless steel. *Journal of Materials Processing Technology* 2001, 118, 442–447.
- [13] Sağlam, H. Frezelemede yapay sinir ağları kullanarak, çok-elemanlı kuvvet ölçümlerine dayalı takım durumu izleme, Doktora Tezi, Selçuk Üniversitesi Mühendislik Fakültesi, Konya, 2000.
- [14] Lo, S. An adaptive-network based fuzzy inference system for prediction of workpiece surface roughness in end milling. *Journal of Materials Processing Technology* 2003, 142, 665–675.
- [15] Öktem, H.; Erzincanlı, F. AISI 1040 çelik malzemenin CNC frezeleme ile işlenmesi sırasında oluşan yüzey pürüzlülüğünün yapay sinir ağıyla modellenmesi. 2. Ulusal Tasarım İmalat ve Analiz Kongresi, 2010, 221–229.
- [16] Asiltürk, I.; Demirci, T.M. Karbür kesici kullanarak sertleştirilmiş AISI 1040 çeliklerin frezelemeindeki yüzey pürüzlülüğünün regresyonla modellenmesi. 2. Ulusal Tasarım İmalat ve Analiz Kongresi, 2010 20–30.
- [17] Kıvık, T. Optimization of surface roughness and flank wear using the Taguchi method in milling of Hadfield steel with PVD and CVD coated inserts. *Measurement*, 2014, 50, 19–28.
- [18] Karabulut Ş.; Güllü, A. An investigation of cutting forces and analytical modelling in milling compacted graphite iron with different lead angles. *Journal of the Faculty of Engineering and Architecture of Gazi University* 2013, 28, 135–143.